Bimagnetic Core/Shell FePt/Fe3O4Nanoparticles

5 AUTHORS, INCLUDING:

Hao Zeng
University at Buffalo, The State University of …
143 PUBLICATIONS 9,072 CITATIONS

SEE PROFILE

Zhihao Wang
Chinese Academy of Sciences
363 PUBLICATIONS 25,667 CITATIONS

SEE PROFILE

Bimagnetic Core/Shell FePt/Fe₃O₄ Nanoparticles

Hao Zeng,[†,§] Jing Li,[‡] Z. L. Wang,[‡] J. P. Liu,[§] and Shouheng Sun*,[†]

IBM T. J. Watson Research Center, Yorktown Heights, New York 10598,
School of Materials Science and Engineering, Georgia Institute of Technology,
Atlanta, Georgia 30332, and Department of Physics, University of Texas at Arlington,
Arlington, Texas 76019

ABSTRACT

Bimagnetic core/shell Fe₅₈Pt₄₂/Fe₃O₄ nanoparticles are synthesized from high-temperature solution phase coating of 4 nm Fe₅₈Pt₄₂ core with Fe₃O₄ shell. The shell is tunable from 0.5 to 3 nm. Magnetic properties of the as-synthesized core/shell particles are dependent on shell thickness due to the exchange coupling between core and shell. Upon reductive annealing, an assembly of the core/shell nanoparticles is transformed into a hard magnetic nanocomposite with enhanced energy product.

Surface modification of nanometer sized inorganic core with different inorganic shell to form core/shell type nanostructures has become an important route to functional nanomaterials. Such modification has brought about interesting physical and chemical properties of the nanostructured materials that have shown important technological applications. The growth of a wide band gap (e.g., ZnS) semiconducting shell around a narrow band gap (e.g., CdSe) core has resulted in core/shell materials with higher luminescence quantum yields than single component semiconductor nanocrystal materials.[1−9] A core/shell type Ag/Au particle possesses not only a strong surface plasma band of Ag between 390 and 420 nm but also a Au surface that allows site-specific binding to various biomolecules and may be used as optic labels for highly sensitive and selective diagnostic detection.[10] Creation of core/shell nanostructures containing metal oxide, such as MgO/Fe₂O₃, CaO/Fe₂O₃, has greatly enhanced the efficiencies of these structures over pure MgO and CaO particles as destructive adsorbents for environmental toxins, such as SO₂ and H₂S.[11,12] Procedures leading to novel inorganic core/shell structures with controlled dimensions on both core and shell and new functionality have also been reported.[13−23]

We report synthesis and characterization of bimagnetic core/shell FePt/Fe₃O₄ nanoparticles with FePt core being 4 nm and shell Fe₃O₄ tunable from 0.5 to 3 nm. We recently demonstrated that using self-assembly of two different magnetic nanoparticles, FePt and Fe₃O₄, followed by reductive annealing to remove organic surfactant around each

nanoparticle, a magnetic nanocomposite FePt−Fe₃Pt could be fabricated.[24] This nanocomposite contains the modulated FePt and Fe₃Pt phases, with the latter having dimension of about 5 nm, leading to effective exchange coupling between FePt hard phase and Fe₃Pt soft phase, and enhanced energy product. However, this binary self-assembly approach requires precise control over the mass ratio and diameters of both the hard and soft magnetic nanoparticles, and the assembly conditions have to be controlled carefully to achieve the intermixing of different phases. A more convenient alternative to controlling the dimension of different phases and achieving the needed intermixing and exchange coupling is using self-assembly of core/shell structured FePt/Fe₃O₄ or Fe₃O₄/FePt nanoparticles. In such system, the dimensions of the hard and soft phases are tuned by the core diameter and shell thickness, and the direct contact between the core and shell ensures strong exchange coupling. Here, we demonstrate that the core/shell structured FePt/Fe₃O₄ nanoparticles, with core and shell being exchange coupled, can be readily synthesized and used as building blocks to form hard magnetic nanocomposites. Magnetic properties of each core/shell nanoparticle can be tuned by varying the thickness of the Fe₃O₄ shell. Such bimagnetic core/shell nanoparticles represent a novel class of nanostructured magnetic materials that will allow precise engineering of magnetic properties by selectively tuning anisotropy, magnetization, and the dimensions of both core and shell, and can further be used to fabricate devices for novel nanomagnetic applications.

The 4 nm Fe₅₈Pt₄₂ nanoparticles were made by the combination of reduction of Pt(acac)₂ and decomposition of Fe(CO)₅ in octyl ether solvent.[25] These 4 nm FePt nanopar-

† IBM T. J. Watson Research Center.
‡ Georgia Institute of Technology.
§ University of Texas at Arlington.

ticles were then used as seeds and mixed with $Fe(acac)_3$ and 1,2-hexadecanediol, oleic acid, and oleylamine in phenyl ether solvent. Fe_3O_4 coating was achieved by heating the mixture as reaction of $Fe(acac)_3$ with 1,2-hexadecanediol, oleic acid and oleylamine at elevated temperature leads to Fe_3O_4.[26] By controlling the material ratio of $Fe(acac)_3$ precursor to FePt nanoparticle seeds, the Fe_3O_4 shell thickness can be readily tuned. An example for making $Fe_{58}Pt_{42}/Fe_3O_4$ with 2 nm Fe_3O_4 shell is as follows:

$Fe(acac)_3$ (1 mmol), 1,2-hexadecanediol (5 mmol), oleic acid (1 mmol) and oleylamine (1 mmol), and phenyl ether (20 mL) were mixed and magnetically stirred under a flow of nitrogen. 50 mg of ~4 nm $Fe_{58}Pt_{42}$ nanoparticles in 5 mL hexane was added. The mixture was heated at 100 °C for 20 min to remove hexane, and then at 200 °C for 1 h. Under a blanket of nitrogen, the mixture was heated to reflux (265 °C) for another 30 min. The black mixture was cooled to room temperature by removing the heat source. Under ambient conditions, ethanol (20 mL) was added to the mixture and a black material was precipitated and separated via centrifugation. The black product was dissolved in hexane (10 mL) in the presence of oleic acid (~0.05 mL) and oleylamine (~0.05 mL), precipitated with ethanol (20 mL) and separated via centrifugation (6000 rpm, 10 min). The product, 4 nm/2 nm FePt/Fe_3O_4 nanoparticles, was redispersed into hexane.

The dimension of core/shell structured nanoparticles was measured using transmission electron microscopy (TEM). Samples for TEM analysis were prepared by drying a hexane dispersion of the particles on amorphous carbon coated copper grids. Particles were imaged using a Philips CM 12 TEM (120 kV). The structure detail of the core/shell nanoparticles was characterized using HRTEM with a JEOL 4000EX at 400 KV. Quantitative elemental EDX analyses of a group of core/shell nanoparticles were carried out with spatially resolved EDX spectrum. X-ray powder diffraction patterns of the particle assemblies were collected on a Siemens D-500 diffractometer under Co Kα radiation (λ = 1.788965 Å). Magnetic studies were carried out using a MPMS2 Quantum Design SQUID magnetometer with fields up to 7 T and temperatures from 5 to 350 K.

Figures 1A and 1B show two typical TEM images of core/shell structured $Fe_{58}Pt_{42}/Fe_3O_4$ nanoparticles, with the darker region in the center being 4 nm $Fe_{58}Pt_{42}$ and the lighter ring being 0.5 nm (Figure 1A) and 2 nm Fe_3O_4 (Figure 1B). The different contrast between the core and shell region is due to the different electron penetration efficiency on metallic FePt and oxide Fe_3O_4. Detailed structure of a single $Fe_{58}Pt_{42}/Fe_3O_4$ particle is characterized with HRTEM, as shown in Figure 1C. The lattice fringes of the shell are clearly shown in the image with adjacent fringe spacing of 0.253 nm, corresponding to {311} lattice planes for Fe_3O_4. Similar HRTEM analysis reveals that the structure of the core is chemically disordered fcc FePt.[27] The images in Figures 1A, 1B, and 1C confirm that the chemically disordered $Fe_{58}Pt_{42}$ core is surrounded by cubic spinel structured Fe_3O_4 shell. EDX analyses of the core/shell nanoparticles reveal that iron content increases with the increase of the shell thickness
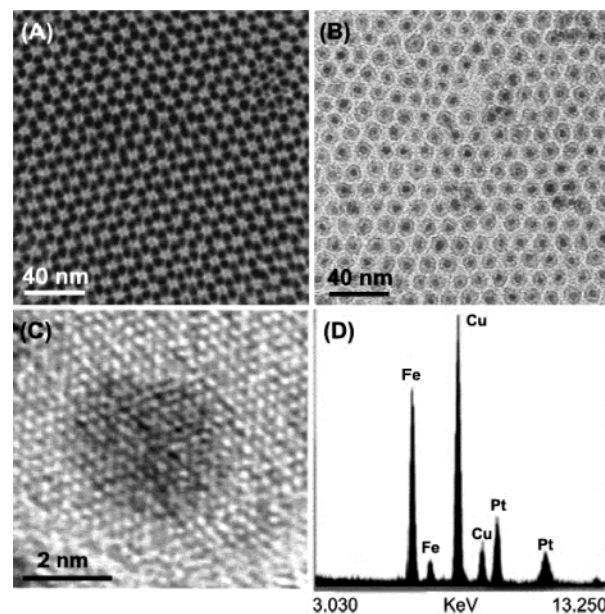

Figure 1. TEM bright field images of core/shell $Fe_{58}Pt_{42}/Fe_3O_4$ nanoparticles with core/shell being (A) 4 nm/0.5 nm and (B) 4 nm/2 nm; (C) HRTEM of a single $Fe_{58}Pt_{42}/Fe_3O_4$ particle with 4 nm core and 2 nm shell; and (D) EDX spectrum of a group of $Fe_{58}Pt_{42}/Fe_3O_4$ nanoparticles with 4 nm core and 1 nm shell. The shell thickness is measured statistically with standard deviation at around 11%.
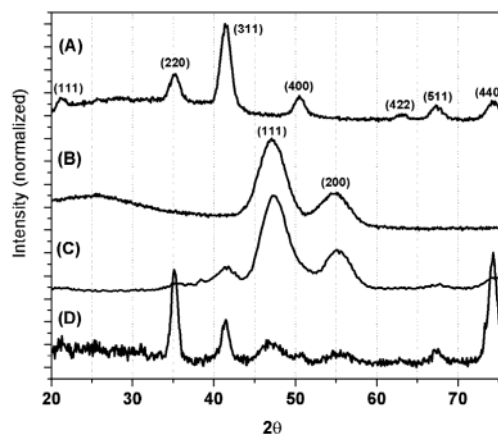
Figure 2. XRD diffraction patterns of the assemblies of (A) 6 nm Fe_3O_4, (B) 4 nm $Fe_{58}Pt_{42}$, (C) 4 nm/1 nm $Fe_{58}Pt_{42}/Fe_3O_4$, and (D) 4 nm/3 nm $Fe_{58}Pt_{42}/Fe_3O_4$ nanoparticles. The assembly was prepared by depositing hexane dispersion of the particles on a glass (A, B) or a Si (100) (C, D) substrate and drying at room temperature.

(see Supporting Information). Figure 1D shows an EDX spectrum from a selected assembly area of the $Fe_{58}Pt_{42}/Fe_3O_4$ nanoparticles with 4 nm core and 1 nm shell. The average composition of these particles is Fe/Pt = 76:24, a ratio larger than the one at 58:42 from the core and is consistent with the presence of 1 nm coating of Fe_3O_4.
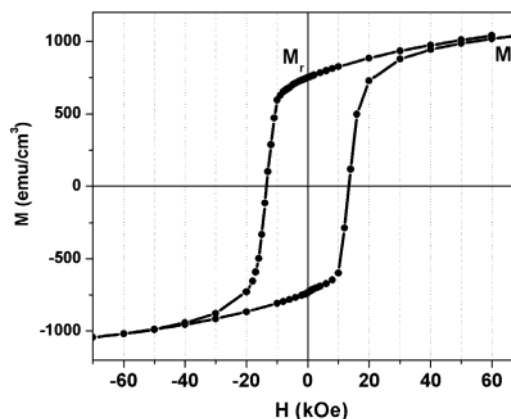
Figure 2 shows the X-ray diffraction (XRD) patterns from the assemblies of cubic spinel structured 6 nm Fe_3O_4 nanoparticles (Figure 2A),[26] chemically disordered fcc 4 nm FePt nanoparticles (Figure 2B),[25] 4 nm/1 nm core/shell structured $Fe_{58}Pt_{42}/Fe_3O_4$ nanoparticles (Figure 2C) and 4 nm/3 nm core/shell structured $Fe_{58}Pt_{42}/Fe_3O_4$ nanoparticles (Figure 2D). Compared with Figures 2A and 2B, Figures
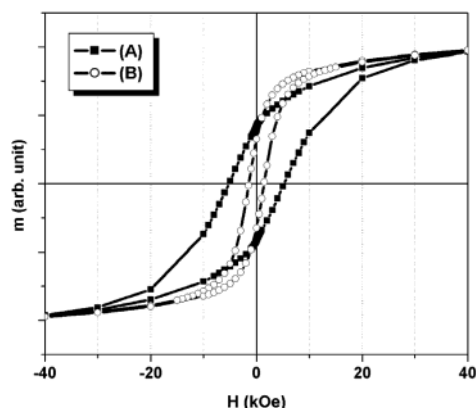
Figure 3. Magnetic hysteresis loops measured at 10 K for Fe_{58}-Pt_{42}/Fe_3O_4 nanoparticles with shell thickness being (A) 0.5 nm and (B) 3 nm, respectively.

Figure 4. Room-temperature magnetic hysteresis loop for the 4 nm/1 nm $Fe_{58}Pt_{42}$/Fe_3O_4 nanoparticle assembly annealed under 5% H_2 + 95% Ar at 650 °C for 1 h.

2C and 2D contain two sets of peaks, with one set matching with that of the chemically disordered fcc FePt and the other cubic spinel structured Fe_3O_4. The diffraction peak width in Figure 2C is broader than that in Figure 2D, indicating that the structure-correlated region of Fe_3O_4 in 1 nm shell is smaller than that in the 3 nm shell. The high intensity from diffraction peaks of (220) and (440) in Figure 2D indicates that reflections from the (220) and (440) planes in Fe_3O_4 shell of the core/shell nanoparticle assemblies are stronger than other planes. The driving force for this preferred alignment is not completely clear at the present time. Study on pure Fe_3O_4 nanoparticle assemblies indicates that if the particles are randomly packed in an assembly, the XRD of such an assembly will show a pattern that resembles the one in Figure 2A. If particles are packed in an ordered array via slow solvent evaporation after particle deposition on a solid surface, the XRD of such a well ordered assembly will show strong (220) and (440) diffraction peaks. This seems to indicate that the (220) and (440) planes in the well ordered self-assembly of Fe_3O_4 nanoparticles prefer a parallel orientation to the substrate surface and further suggests that the core/shell structured FePt/Fe_3O_4 nanoparticles form a well ordered array with the (220) and (440) planes in Fe_3O_4 shell being close to parallel to the substrate.

As synthesized, the $Fe_{58}Pt_{42}$/Fe_3O_4 core/shell nanoparticles are ferromagnetic at low temperatures but superparamagnetic at room temperature. Figure 3 shows the hysteresis loops, measured at 10 K, of the particles with shell thickness being 0.5 and 2 nm, respectively. The particles with 0.5 nm Fe_3O_4 shell have coercivity (H_c) of 5 kOe, while those with 3 nm shell have a H_c value of only 1.4 kOe, indicating the dependence of H_c over the thickness of the Fe_3O_4 shell. The large H_c value of the core/shell nanoparticles originates from low-temperature hard magnetic properties of the $Fe_{58}Pt_{42}$ core, as the coercivity of the as-synthesized 4 nm $Fe_{58}Pt_{42}$ nanoparticles is 5.5 kOe at 10 K. Fe_3O_4 is magnetically a much softer material, with 10 K H_c ranging from 200 Oe for 4 nm to 450 Oe for 16 nm nanoparticles. However, in $Fe_{58}Pt_{42}$/Fe_3O_4 system, the magnetic behaviors of $Fe_{58}Pt_{42}$ and Fe_3O_4 are not distinguishable, and the hysteresis loops measured at 10 K show smooth change of magnetization with

applied field, suggesting that $Fe_{58}Pt_{42}$ core and Fe_3O_4 shell are in intimate contact and are exchange-coupled.[28] Therefore the magnetization directions of both core and shell switch coherently under an external magnetic field.

The exchange-coupled FePt/Fe_3O_4 nanoparticles can be used as building blocks to form hard magnetic nanocomposites with enhanced magnetic properties. Upon reductive annealing under 5% H_2 + 95% Ar at 650 °C for 1h, the assembly of $Fe_{58}Pt_{42}$/Fe_3O_4 nanoparticles was transformed into a nanocomposite with hard magnetic properties at room temperature. A room-temperature hysteresis loop of the annealed 4 nm/1 nm $Fe_{58}Pt_{42}$/Fe_3O_4 assembly is given in Figure 4 with H_c measured to be 13.5 kOe and saturation magnetization M_s to be 1040 emu/cc. This M_s is higher than that (~950 emu/cc) from the $Fe_{58}Pt_{42}$ nanoparticle assembly annealed under the same condition, suggesting that in the annealed $Fe_{58}Pt_{42}$/Fe_3O_4 nanoparticle assembly there exists a higher moment iron-rich species that contributes to the overall magnetization increase in the composite. Further, the hysteresis loop in Figure 4 shows a smooth magnetization transition and a remanence ratio M_r/M_s value of about 0.73, the behavior similar to the nanocomposite obtained from $Fe_{58}Pt_{42}$ and Fe_3O_4 binary assembly,[24] indicating effective exchange coupling between the hard and soft phases.[28] As a comparison, annealing an assembly containing iron rich $Fe_{70-80}Pt_{30-20}$ alloy nanoparticles led to materials that are magnetically much softer (H_c less than 1 kOe)[29] than the composite from 4 nm/1 nm $Fe_{58}Pt_{42}$/Fe_3O_4 nanoparticle assembly with average composition of $Fe_{76}Pt_{24}$. This suggests that the hard magnetic property of the annealed core/shell assembly originates from exchange-coupled hard and soft phases, not from homogeneous iron-rich FePt alloy. The energy product ($(BH)_{max}$), which describes the magneto-static energy stored in a magnet and defined as the maximum B−H product in the second quadrant of a B−H loop, where B = H + $4\pi M$, can be obtained from the hysteresis measurement.[30] The $(BH)_{max}$ based on the M−H loop in Figure 4 is 18 MGOe, a value that is a 38% increase over the theoretical value of 13 MGOe from the nonexchange-coupled isotropic FePt bulk materials,[31] indicating the core/shell structured

FePt/Fe$_3$O$_4$ nanoparticles can indeed be used as building blocks to form nanocomposites with enhanced magnetic properties.

This report demonstrates that magnetic core/shell structured Fe$_{58}$Pt$_{42}$/Fe$_3$O$_4$ nanoparticles can be made from high-temperature solution phase coating of 4 nm Fe$_{58}$Pt$_{42}$ core with Fe$_3$O$_4$ shell. Magnetic properties of the core/shell particles can be engineered by tuning the shell thickness. Upon reductive annealing, this core/shell structure can be transformed into hard magnetic nanocomposite with enhanced energy products. Our further experiments indicate that the synthetic approach reported here can be extended to produce a rich variety of magnetic core/shell systems. With proper choice of materials and dimension tuning of both core and shell, these core/shell nanoparticles may be used as building blocks for creation of novel functional nanomaterials for various magnetic applications.

Supporting Information Available: One figure: (S1) EDX spectra of core/shell Fe$_{58}$Pt$_{42}$/Fe$_3$O$_4$ nanoparticles with core being 4 nm and shell being 2 and 3 nm, respectively. This material is available free of charge via the Internet at http://pubs.acs.org.

References

(1) Kortan, A. R.; Hull, R.; Opila, R. L.; Bawendi, M. G.; Steigerwald, M. L.; Carrol, P. J.; Brus, L. E. *J. Am. Chem. Soc*. **1990**, *112*, 1327.
(2) Hasselbarth, A.; Eychmuller, A.; Eichburger, R.; Giesi, M.; Mews, A.; Weller, H. *J. Phys. Chem. B* **1993**, *97*, 5333.
(3) Zhou, H. S.; Honma, I.; Sasahara, H.; Komiyama, H.; Kraus, J. W. *Chem. Mater*. **1994**, *6*, 1534.
(4) Danek, M.; Jensen, K. F.; Murray, C. B.; Bawendi, M. G. *Chem. Mater*. **1996**, *8*, 173.
(5) Hines, M. A.; Guyot-Sionnest, P. *J. Phys. Chem. B* **1996**, *100*, 468.
(6) Dabbousi, B. O.; Rodriguez-Viejo, J.; Mikulec, F. V.; Heine, J. R.; Mattoussi, H.; Ober, R.; Jensen, K. F.; Bawendi, M. G. *J. Phys. Chem. B* **1997**, *101*, 9463.
(7) Peng, X.; Schlamp, M. C.; Kadavanich, A. V.; Alivisatos, A. P *J. Am. Chem. Soc.* **1997**, *119*, 7019.
(8) Malik, M. A.; O'Brien, P.; Revaprasadu, N. *Chem. Mater.* **2002**, *14*, 2004.
(9) Reiss, P.; Bleuse, J.; Pron, A. *Nano Lett.* **2002**, *2*, 781.
(10) Cao, Y.; Jin, R.; Mirkin, C. A. *J. Am. Chem. Soc.* **2001**, *123*, 7961.
(11) Decker, S.; Klabunde, K. J. *J. Am. Chem. Soc.* **1996**, *118*, 12465.
(12) Carnes, C. L.; Klabunde, K. J. *Chem. Mater.* **2002**, *14*, 1806.
(13) Pastoriza-Santos, I.; Koktysh, D. S.; Mamedov, A. A.; Giersig, M.; Kotov, N. A.; Liz-Marzán, L. M. *Langmuir* **2000**, *16*, 2731.
(14) Westcott, S. L.; Averitt, R. D.; Wolfgang, J. A.; Nordlander, P.; Halas, N. J. *J. Phys. Chem. B* **2001**, *105*, 9913.
(15) Lu, Y.; Yin, Y.; Mayers, B. T.; Xia, Y. *Nano Lett.* **2002**, *2*, 183.
(16) Yin, Y.; Lu, Y.; Sun, Y.; Xia, Y. *Nano Lett.* **2002**, *2*, 427.
(17) Lu, Y.; Yin, Y.; Li, Z.; Xia, Y. *Nano Lett.* **2002**, *2*, 785.
(18) Vestal, C. R.; Zhang, Z. J. *J. Am. Chem. Soc.* **2002**, *124*, 14312.
(19) Teng, X.; Black, D.; Watkins, N.; Gao, Y.; Yang, H. *Nano Lett.* **2003**, *3*, 261.
(20) Wang, Y.; Teng, X.; Wang J.; Yang, H. *Nano Lett.* **2003**, *3*, 789.
(21) Carpenter, E. E.; Calvin, S.; Stroud, R. M.; Harris, V. G. *Chem. Mater.* **2003**, *15*, 3245.
(22) Sobal, N. S.; Ebel, U.; Möhwald, H.; Giersig, M. *J. Phys. Chem. B* **2003**, *107*, 7351.
(23) Skumryev, V.; Stoyanov, S.; Zhang, Y.; Hadjipanayis, G.; Givord, D.; Nogues, J. *Nature* **2003**, *423*, 850.
(24) Zeng, H.; Li, J.; Wang, Z. L.; Liu, J. P.; Sun, S. *Nature* **2002**, *420*, 395.
(25) Sun, S.; Murray, C. B.; Weller, D.; Folks, L.; Moser, A. *Science* **2000**, *287*, 1989.
(26) Sun, S.; Zeng, H. *J. Am. Chem. Soc.* **2002**, *124*, 8204.
(27) Dai, Z. R.; Sun, S.; Wang, Z. L. *Surf. Sci.* **2002**, *505*, 325.
(28) Preliminary TEM studies suggest that the hard phase is FePt while the soft phase is close to Fe$_3$Pt as shown in ref 24. Detailed structural and magnetic analyses on this new type of nanocomposite, along with the one from Fe$_3$O$_4$/FePt nanoparticle assembly, are on the way.
(29) Sun, S.; Fullerton, E. E.; Weller, D.; Murray, C. B. *IEEE Trans. Magn.* **2001**, *37*, 1239.
(30) O'Handley, R. C. *Modern Magnetic Materials − Principles and Applications*; John Wiley & Sons: New York, 2000; pp 437−514.
(31) Klemmer, T.; Hoydick, D.; Okamura, H.; Zhang, B.; Soffa, W. A. *Scripta Met.* **1995**, *33*, 1793.

NL035004R